A GTD-BASED BOUNDARY ELEMENT METHOD FOR A SURFACE SCATTERING PROBLEM

S. Langdon — School of Mathematics, University of New South Wales, Sydney, NSW 2052, Australia
S.N. Chandler-Wilde — Department of Mathematics, University of Reading, Whiteknights, PO Box 220, Berkshire RG6 6AX, U.K.

1 INTRODUCTION

This paper is concerned with the problem of acoustic scattering of an incident wave by a planar surface with spatially varying acoustical surface impedance. In the case in which there is no variation in the acoustical properties of the surface or the incident field in some fixed direction parallel to the surface, the problem is effectively two-dimensional. Adopting Cartesian coordinates $0x_1x_2x_3$, let this direction be that of the x_3-axis and the surface be the plane $x_2 = 0$, with the wave incident from the half-space $x_2 > 0$. Under the further assumption that the incident wave and scattered fields are time harmonic, the total acoustic field satisfies the Helmholtz equation

$$\Delta u^t + k^2 u^t = 0, \quad \text{in the upper half-plane } U := \{x = (x_1, x_2) : x_2 > 0\}, \tag{1}$$

supplemented with the impedance boundary condition

$$\frac{\partial u^t}{\partial x_2} + \mathrm{i}k\beta u^t = 0, \quad \text{on the boundary } \Gamma := \{(x_1, 0) : -\infty < x_1 < \infty\}, \tag{2}$$

where $k = \omega/c > 0$, with $\omega = 2\pi\mu$, μ is the frequency of the incident wave and c is the speed of sound in U. The acoustic pressure at time t, position (x_1, x_2, x_3) is then given by $\mathrm{Re}(\mathrm{e}^{-\mathrm{i}\omega t}u^t(x))$, for $x = (x_1, x_2) \in \overline{U} := U \cup \Gamma$.

For the problem of outdoor sound propagation over inhomogeneous flat terrain, the function β in (2) is the relative ground surface admittance, which is, in general, a function of both frequency and ground surface type. There is no space here to discuss specific expressions for β for a variety of outdoor surfaces (see e.g. [1]), but note that any physically appropriate impedance model satisfies $\mathrm{Re}\beta \geq 0$ (to ensure that the ground surface absorbs rather than emits energy) and, for a perfectly rigid surface, $\beta \equiv 0$. Here, we assume throughout that β is piecewise constant, and constant outside some finite interval $[a, b]$, so that for some real numbers $a = t_0 < t_1 < \ldots < t_n = b$, the admittance at point $(x_1, 0)$ on Γ is given by

$$\beta(x_1) = \begin{cases} \beta_j, & x_1 \in (t_{j-1}, t_j], \\ \beta_c, & x_1 \in \mathbb{R}\backslash(t_0, t_n], \end{cases}$$

as shown in figure 1. We also assume that, for some $\epsilon > 0$,

$$\mathrm{Re}\beta_c \geq \epsilon, \quad \mathrm{Re}\beta_j \geq \epsilon, \quad |\beta_c| \leq \epsilon^{-1}, \quad |\beta_j| \leq \epsilon^{-1}, \quad j = 1, \ldots, n. \tag{3}$$

For simplicity of exposition, we restrict our attention to the case of plane wave incidence, so that the incident field u^i is given by

$$u^i(x) = \exp[\mathrm{i}k(x_1 \sin\theta - x_2 \cos\theta)], \tag{4}$$

where $-\pi/2 < \theta < \pi/2$ is the angle of incidence. The reflected or scattered part of the wave field $u := u^t - u^i$.

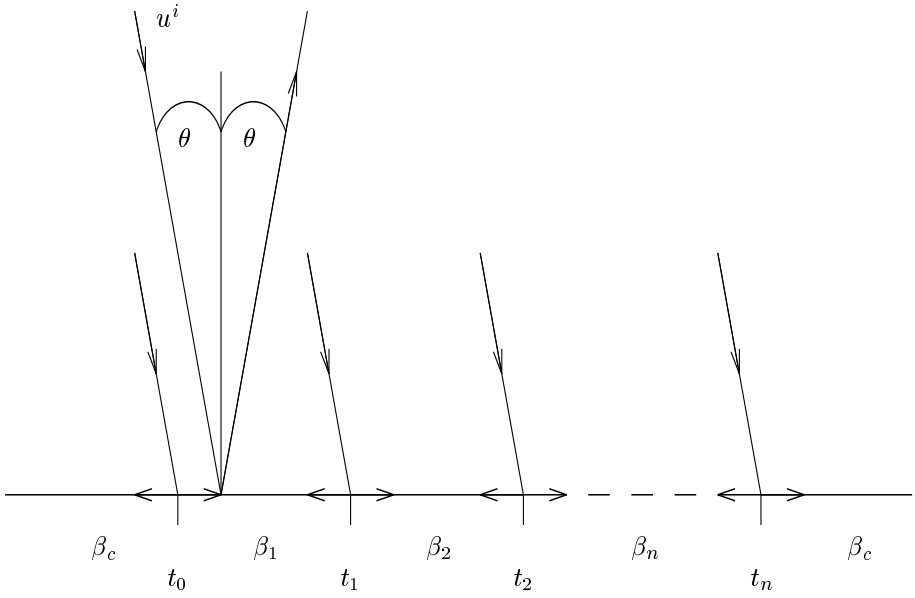

Figure 1: Acoustic scattering by an impedance boundary. Typical incident and reflected rays are shown as well as some of the rays arising from diffraction at impedance discontinuities.

In this paper, we are concerned with solving (1)–(2) numerically specifically in the case in which k may be large. This corresponds to the high frequency, low wavelength case (the wavelength is $\lambda = c/\mu = 2\pi/k$) and presents a number of numerical difficulties. Standard finite or boundary element schemes for scattering problems become prohibitively expensive as $k \to \infty$, with a fixed number of elements being required per wavelength in order to achieve reasonable accuracy. When the wavelength is short compared to the size of the obstacle this leads to excessively large systems of equations. Much recent work has focused on enriching the approximation space with plane wave solutions of (1), in order to more efficiently represent the highly oscillatory solution. Although excellent numerical results have been reported, until recently there has been little in the way of error analysis for this approach, specifically with regard to the dependence of the error estimates on the wavenumber k. For a full discussion and literature review regarding this approach we refer to [4].

Here we use similar ideas, to propose a numerical scheme for which we can establish convergence, uniformly in k, as the number of degrees of freedom tends to infinity. Thus, any required accuracy can be achieved by solving a linear system whose size is fixed for all wavenumbers k. To achieve this, we begin by using ideas in the spirit of the geometrical theory of diffraction (GTD) to obtain representations for the solution on the boundary. These representations can be viewed as explicitly summing the reflected and diffracted ray path contributions to the field on the boundary shown in figure 1. Precisely we identify and subtract off the leading order behaviour on each interval (namely the incident and reflected rays) as $k \to \infty$. The remaining scattered wave (consisting of the rays diffracted at impedance discontinuities) can then be expressed (on the boundary Γ) as the product of the known oscillatory functions $\mathrm{e}^{\pm \mathrm{i}kx_1}$ and unknown non-oscillatory functions denoted as $f_j^{\pm}$, whose high order derivatives can be shown to decay quickly away from impedance discontinuities. We then use a Galerkin boundary element method with a graded mesh, obtaining piecewise polynomial (degree ν) representations of the non-oscillatory functions $f_j^{\pm}$.

This approach was first used in [2], leading to an error bound depending only logarithmically on the wavenumber k. This has been improved upon in [4], where stronger bounds on $f_j^{\pm}$ have been proved,

leading to a slightly different approximation space. For this scheme it was shown in [4] that the error in computing an approximation to the total wave field is of order $N^{-(\nu+1)} \log^{1/2} |\min(N,k)|$ when the total number of degrees of freedom is proportional to $N \log |\min(N,k)|$. In §2 we briefly describe the Galerkin boundary element method approach of [4], and we present the regularity and error estimates proved there. In §3 we describe the implementation of the scheme. The main new results of this paper are contained in §4, where we present numerical results in the case that $\theta \approx \pi/2$, i.e. for a grazing angle of incidence. We demonstrate that even in this case the number of degrees of freedom required in order to achieve a prescribed level of accuracy remains bounded as $k \to \infty$. We also show via numerical results that the bounds of §2, which describe the rate of decay of the diffracted rays along the boundary, seem to be sharp. Finally in §5 we present some conclusions.

2 THE BOUNDARY ELEMENT METHOD AND ERROR ESTIMATES

It is shown in [4] that the boundary value problem (1)–(2), accompanied by an appropriate radiation condition, can be reformulated as the second kind boundary integral equation

$$\phi = \psi_{\beta_c} + K_\beta^{\beta_c} \phi, \tag{5}$$

where for $s \in \mathbb{R}$, $\phi(s) := u^t((s/k,0))$ is the total field at point $(s/k,0)$ on Γ, $\psi_{\beta_c}(s) := (2\cos\theta/[\cos\theta + \beta_c]) \exp(\mathrm{i}s\sin\theta)$ is the total acoustic field at the same point in the case that the surface has constant impedance β_c, and

$$K_\beta^{\beta_c}\chi(s) := \mathrm{i}\int_{ka}^{kb} G_{\beta_c}((s/k,0),(t/k,0))(\beta(t/k)-\beta_c)\chi(t)\,dt,$$

with $G_{\beta_c}(x,y)$ denoting the Green's function for (1)–(2). We refer to [4] for details. Our numerical scheme for solving (5) is based on a consideration of the contribution of the reflected and diffracted ray paths in the spirit of the geometrical theory of diffraction (GTD). In particular, to leading order as $k \to \infty$, on the interval (t_{j-1}, t_j) it seems reasonable to suppose that the total field $\phi \approx \psi_{\beta_j}$, the total field there would be if the whole boundary had the admittance β_j of the interval (t_{j-1}, t_j). In fact, for $s \neq \tilde{t}_j := kt_j$, $j = 0, \ldots, n$, it follows from theorem 2.1 below that $\phi(s) \to \Psi(s)$ as $k \to \infty$, where $\Psi(s) := \psi_{\beta_j}(s)$, $s \in (\tilde{t}_{j-1}, \tilde{t}_j]$, $j = 1, \ldots, n$, and $\Psi(s) := \psi_{\beta_c}(s)$, $s \in R\backslash(\tilde{t}_0, \tilde{t}_n]$. In our numerical scheme we compute the difference between ϕ and Ψ,

$$\Phi(s) := \phi(s) - \Psi(s) = \Psi_{\beta_c}(s) + K_\beta^{\beta_c}\Phi(s), \quad s \in \mathbb{R}. \tag{6}$$

where Ψ_{β_c} is known and is given by $\Psi_{\beta_c} := \psi_{\beta_c} - \Psi + K_\beta^{\beta_c}\Psi$. Equation (6) will be the integral equation that we solve numerically, and we approximate its solution by $\Phi_N \in V_{\Omega,\nu}$, defined by the Galerkin method equation

$$(\Phi_N, \chi) = (\Psi_{\beta_c}, \chi) + (K_\beta^{\beta_c}\Phi_N, \chi), \quad \text{for all } \chi \in V_{\Omega,\nu}, \tag{7}$$

where the inner product $(\cdot,\cdot)$ is defined by $(f,g) = \int_{-\infty}^{\infty} f(s)g(s)\,\mathrm{d}s$. The key to achieving a good approximation with a small number of degrees of freedom lies in choosing the approximation space $V_{\Omega,\nu}$ appropriately . We begin by writing

$$\Phi(s) = e^{\mathrm{i}s} f_j^+(s - \tilde{t}_{j-1}) + e^{-\mathrm{i}s} f_j^-(\tilde{t}_j - s), \quad s \in (\tilde{t}_{j-1}, \tilde{t}_j],\ j = 1, \ldots, n. \tag{8}$$

In GTD terms, the first term in (8) is an explicit summation of all the diffracted rays scattered at the discontinuities in impedance at $\tilde{t}_{j-1}$ which travel from left to right along $(\tilde{t}_{j-1}, \tilde{t}_j)$. Similarly, the other term in (8) is the contribution to the diffracted field diffracted by the discontinuity at $\tilde{t}_j$. These diffracted rays are illustrated in figure 1. It is shown in [4] that the functions $f_j^\pm$ are not oscillatory, and that they decay rapidly away from discontinuities in impedance. Specifically the following bounds on $f_j^\pm$ and their derivatives are shown:

Theorem 2.1 *Suppose (3) holds for some $\epsilon > 0$. Then for $r > 1$, $j = 0, \ldots, n$, $m = 0, 1, \ldots,$, there exist constants $C_{m,\epsilon}$, dependent only on m and ϵ, such that*

$$\left| {f_{j+1}^{+}}^{(m)}(r) \right|, \left| {f_{j}^{-}}^{(m)}(r) \right| \leq C_{m,\epsilon} r^{-1/2-m} \cos\theta, \tag{9}$$

and there exists a constant C_ϵ, dependent only on ϵ, such that

$$\left| f_{j+1}^{+}(r) \right|, \left| f_{j}^{-}(r) \right| \leq C_\epsilon \frac{r^{-3/2} n^3}{\cos\theta}. \tag{10}$$

We shall show via numerical experiments in §4 that, for $m = 0$, these bounds appear to be sharp with respect to θ and r.

We then seek a piecewise polynomial approximation to $f_j^{\pm}$ on a graded mesh. For $j = 1, \ldots, n$ we define

$$A_j := \min\left\{ \alpha \frac{n^3 N^{\nu+1}}{\cos\theta}, \tilde{t}_j - \tilde{t}_{j-1} \right\},$$

where $N = 2, 3, \ldots$, and $\alpha \geq 1$ is an absolute constant (chosen experimentally). Assuming $A_j > 1$, the mesh $\Lambda_{N,A_j} : 0 = y_0 < \ldots < y_{N+N_{A_j}} = A_j$ is a composition of two parts and consists of the points

$$y_i := \begin{cases} (i/N)^{1+2\nu/3}, & i = 0, \ldots, N, \\ A_j^{(i-N)/N_{A_j}}, & i = N+1, \ldots, N+N_{A_j}, \end{cases}$$

with $N_{A_j} = \lceil -\log A_j / [q \log(1 - 1/N)] \rceil$ chosen to ensure a smooth transition between the two parts of the mesh. For $j = 1, \ldots, n$ we then define the two meshes $\Omega_j^+ := \tilde{t}_{j-1} + \Lambda_{N,A_j}$, $\Omega_j^- := \tilde{t}_j - \Lambda_{N,A_j}$. Letting $e_\pm(s) := \mathrm{e}^{\pm \mathrm{i}s}$, $s \in \mathbb{R}$, we then define $V_{\Omega_j^+,\nu} := \{\sigma e_+ : \sigma \in \Pi_{\Omega_j^+,\nu}\}$, $V_{\Omega_j^-,\nu} := \{\sigma e_- : \sigma \in \Pi_{\Omega_j^-,\nu}\}$, for $j = 1, \ldots, n$, where

$$\begin{aligned} \Pi_{\Omega_j^+,\nu} &:= \{\sigma|_{(\tilde{t}_{j-1}+y_{m-1}, \tilde{t}_{j-1}+y_m)} \text{ is a polynomial of degree} \leq \nu, \text{ for} \\ &\qquad m = 1, \ldots, N + N_{A_j}, \text{ and } \sigma|_{\mathbb{R}\setminus[\tilde{t}_{j-1}, \tilde{t}_{j-1}+A_j]} = 0\}, \\ \Pi_{\Omega_j^-,\nu} &:= \{\sigma|_{(\tilde{t}_j - y_m, \tilde{t}_j - y_{m-1})} \text{ is a polynomial of degree} \leq \nu, \text{ for} \\ &\qquad m = 1, \ldots, N + N_{A_j}, \text{ and } \sigma|_{\mathbb{R}\setminus[\tilde{t}_j - A_j, \tilde{t}_j]} = 0\}. \end{aligned}$$

Our approximation space is then $V_{\Omega,\nu}$, the linear span of $\bigcup_{j=1,\ldots,n}\{V_{\Omega_j^+,\nu} \cup V_{\Omega_j^-,\nu}\}$. The number of degrees of freedom, i.e. $M_N := \dim(V_{\Omega,\nu})$ is bounded by $M_N \leq CN\log(\min(N,k))$, where C does not depend on N or k.

We will discuss some implementation details of the scheme in §3, but we conclude this section by stating our error estimates. Under the assumption

$$|\beta_j - \beta_c| < \mathrm{Re}\beta_c, \quad j = 1, \ldots, n, \tag{11}$$

the following theorem is proved in [4]. We remark also that numerical results in [3] suggest that these error estimates hold even if (11) does not hold, provided (3) still holds.

Theorem 2.2 *If (3) holds for some $\epsilon > 0$, and (11) is satisfied, then there exist constants $C_1, C_2 > 0$ dependent only on ν and ϵ such that*

$$\begin{aligned} \|\Phi - \Phi_N\|_{2,(\tilde{a},\tilde{b})} &\leq \frac{C_1 n^{1/2}(1 + \log^{1/2}(\min(\alpha n^3 N^{\nu+1}/\cos\theta, k(b-a))))}{(\mathrm{Re}\beta_c - \|\beta - \beta_c\|_\infty) N^{\nu+1}}, \\ |u^t(x) - u_N^t(x)| &\leq \frac{C_2 n^{1/2}(1 + \log^{1/2}(\min(\alpha n^3 N^{\nu+1}/\cos\theta, k(b-a))))}{(\mathrm{Re}\beta_c - \|\beta - \beta_c\|_\infty) N^{\nu+1}}, \end{aligned}$$

for $x \in \overline{U}$, where $u_N^t(x)$ is the approximation to u^t defined by

$$u_N^t(x) := u_{\beta_c}^t(x) + \mathrm{i}k \int_{t_0}^{t_n} G_{\beta_c}(x,(y_1,0))(\beta(y_1)-\beta_c)\phi_N(ky_1)\,\mathrm{d}y_1,$$

with $\phi_N := \Phi_N + \Psi$.

3 IMPLEMENTATION

In this rest of this paper we consider only the case $\nu = 0$ and $n = 1$, but remark that the implementation of the scheme is similar for larger values of ν and n. Recalling (7), the equation we wish to solve is

$$(\Phi_N, \rho) - (K_\beta^{\beta_c}\Phi_N, \rho) = (\Psi_\beta^{\beta_c}, \rho), \quad \text{for all } \rho \in V_{\Omega,0}. \tag{12}$$

Writing Φ_N as a linear combination of basis functions of $V_{\Omega,0}$, we have $\Phi_N(s) = \sum_{j=1}^{M_N} v_j \rho_j(s)$, where

$$M_N = 2(N + N_{A_1}) \le 2N\,(3/2 + \log(\alpha/\cos\theta) + \log N) \tag{13}$$

is the number of degrees of freedom and ρ_j is the j^{th} basis function, defined by

$$\begin{aligned}
\rho_j(s) &:= \frac{\mathrm{e}^{\mathrm{i}s}\chi_{[t_0+y_{j-1},t_0+y_j)}(s)}{(y_j - y_{j-1})^{1/2}}, \quad j = 1,\ldots,N+N_{A_1},\\
\rho_{j+N+N_{A_1}}(s) &:= \frac{\mathrm{e}^{-\mathrm{i}s}\chi_{[t_1-y_j,t_1-y_{j-1})}(s)}{(y_j - y_{j-1})^{1/2}}, \quad j = 1,\ldots,N+N_{A_1},
\end{aligned}$$

where $\chi_{[s_1,s_2)}$ denotes the characteristic function of the interval $[s_1,s_2)$, so that $\chi_{[s_1,s_2)}(s) = 1$ if $s_1 \le s < s_2$, $= 0$ otherwise.

Equation (12) then becomes the linear system

$$\sum_{j=1}^{M_N} v_j((\rho_j,\rho_m) - (K_\beta^{\beta_c}\rho_j,\rho_m)) = (\Psi_\beta^{\beta_c},\rho_m), \quad m = 1,\ldots,M_N. \tag{14}$$

Formulae for the coefficients of this linear system are given in [3]; some integrals must be evaluated numerically but these integrals do not increase in difficulty as $k \to \infty$. Furthermore, it is shown in [4] that the linear system is well conditioned, with the conditioning improving as $k \to \infty$.

4 NUMERICAL RESULTS WITH A GRAZING ANGLE OF INCIDENCE

In this section we investigate the behaviour of our scheme when the angle of incidence is close to grazing, i.e. $\theta = \pi/2 - \varepsilon$ for $\varepsilon \ll 1$. As our numerical example, we take $n = 1$,

$$\beta(s) = \begin{cases} 0.505 - 0.3\mathrm{i}, & s \in [-m\lambda, m\lambda],\\ 1 & s \notin [-m\lambda, m\lambda], \end{cases}$$

for m=5, 10, 160, and 5120 where $k = 1$ and $\lambda = 2\pi$ is the wavelength. This experiment is equivalent to fixing the interval $[a,b] = [t_0,t_1]$ and decreasing the wavelength. Assumption (11) is satisfied, so we would expect theorem 2.2 to hold.

For $\varepsilon = 0.1$ and $\varepsilon = 10^{-4}$, and for $m = 10$, $m = 160$ and $m = 5120$, we compute Φ_N with $\nu = 0$, $\alpha = 40$ and N=2, 4, 8, 16, 32. For the purpose of computing errors, we compute the "exact" solution

		$\varepsilon = 0.1$,			$\varepsilon = 10^{-4}$		
$(b-a)/\lambda$	N	M_N	$\|\Phi_N - \Phi\|_2/\|\Phi\|_2$	EOC	M_N	$\|\Phi_N - \Phi\|_2/\|\Phi\|_2$	EOC
20	2	18	1.6979×10^{-1}	1.66	18	9.7846×10^{-2}	1.28
	4	42	5.3834×10^{-2}	1.14	42	4.0404×10^{-2}	1.14
	8	90	2.4473×10^{-2}	1.03	90	1.8332×10^{-2}	1.04
	16	182	1.1992×10^{-2}	0.98	182	8.9401×10^{-3}	0.99
	32	370	6.0633×10^{-3}		370	4.5135×10^{-3}	
320	2	24	1.3951×10^{-1}	1.24	26	9.9251×10^{-2}	1.28
	4	60	5.8936×10^{-2}	1.13	62	4.0851×10^{-2}	1.07
	8	130	2.6919×10^{-2}	1.04	130	1.9438×10^{-2}	1.04
	16	268	1.3093×10^{-2}	1.00	268	9.4427×10^{-3}	1.00
	32	544	6.5581×10^{-3}		544	4.7315×10^{-3}	
5120	2	24	1.4287×10^{-1}	1.18	36	9.9223×10^{-2}	1.27
	4	60	6.2884×10^{-2}	1.03	86	4.1084×10^{-2}	1.05
	8	138	3.0751×10^{-2}	1.04	182	1.9827×10^{-2}	1.06
	16	304	1.4953×10^{-2}	1.08	376	9.5356×10^{-3}	1.04
	32	660	7.0871×10^{-3}		762	4.6269×10^{-3}	

Table 1: $\|\Phi - \Phi_N\|_2/\|\Phi\|_2$ for $\varepsilon = 0.1$, 10^{-4}, m=10, 160 and 5120, and increasing N.

Φ with $N = 128$ and $\alpha = 1000$. The relative L_2 errors $\|\Phi - \Phi_N\|_2/\|\Phi\|_2$ are shown in table 1. (We approximate $\|\cdot\|_2$ by the discrete L_2 norm, sampling at 100000 evenly spaced points in the relevant interval for the function whose norm is to be evaluated.) The estimated order of convergence is given by $\text{EOC} := \log_2(\|\Phi - \Phi_N\|_2/\|\Phi - \Phi_{2N}\|_2)$. From theorem 2.2 we would expect EOC ≈ 1, and this is what we see. For $\varepsilon = 10^{-4}$, $\alpha/\cos\theta \approx 400000$, whereas for $\varepsilon = 0.1$, $\alpha/\cos\theta \approx 400$. Recalling (13), we would thus expect the number of degrees of freedom to be greater for $\varepsilon = 10^{-4}$ than for $\varepsilon = 0.1$, and this is indeed what we see when m is large. For fixed N and m, there exists $\tilde{\varepsilon}$ such that for all $\varepsilon < \tilde{\varepsilon}$, $\alpha N/\cos\theta$ will be greater than $\tilde{t}_j - \tilde{t}_{j-1}$, in which case, the graded mesh will extend over the whole interval $[\tilde{t}_{j-1}, \tilde{t}_j]$. While this is true, the number of degrees of freedom will increase logarithmically with respect to m as m increases, until m is sufficiently large that $\tilde{t}_j - \tilde{t}_{j-1} > \alpha N/\cos\theta$. So, for all ε it is true that the number of degrees of freedom needed to maintain accuracy remains bounded as $m \to \infty$, but the size of this bound grows as $\varepsilon \to 0$.

Recalling theorem 2.1, when $\theta \approx \pi/2$ so that $\cos\theta \approx 0$ we would expect $|\Phi(s)|/\cos\theta$ to decay like $s^{-1/2}$ away from the impedance discontinuities, and when $\theta \not\approx \pi/2$ we would expect $|\Phi(s)|$ to decay like $s^{-3/2}$ away from the impedance discontinuities. In figure 2 we plot $|\Phi(s)|$ for $m = 5120$ and $\varepsilon = 0.1$. For comparison we also plot $(s-t_0)^{-1/2}$ and $(s-t_0)^{-3/2}$ on the same graph. Clearly, $|\Phi(s)|$ decays like $(s-t_0)^{-3/2}$, away from the impedance discontinuities. In figure 3 we plot $|\Phi(s)|/\cos\theta$ for $m = 5120$ and $\varepsilon = 10^{-4}$. For comparison we also plot $(s-t_0)^{-1/2}$ and $(s-t_0)^{-3/2}$ on the same graph. We now see that $|\Phi(s)|/\cos\theta$ decays like $(s-t_0)^{-1/2}$, away from the impedance discontinuities, which is what we might expect as $\theta \approx \pi/2$. This suggests that the bounds of theorem 2.1 are sharp with respect to r and θ.

In figures 4–9 we plot the incident, scattered and total wave fields for $m = 5$ (so that $b - a = 10\lambda$) and for $\varepsilon = 0.4$, 0.2, 0.1, 0.05, 0.01 and 10^{-4}, where $\theta = \pi/2 - \varepsilon$, all computed with $N = 16$. In each plot, we also show $\text{Re}u^t - \text{Re}u_1^t$, i.e. the total wave field minus what the total wave field would be in the case that $\beta \equiv 1$. This last plot allows us to see the diffracted rays more clearly. As θ gets close to $\pi/2$ the incident and reflected fields cancel each other out near the surface. The diffracted rays can be clearly seen in each case.

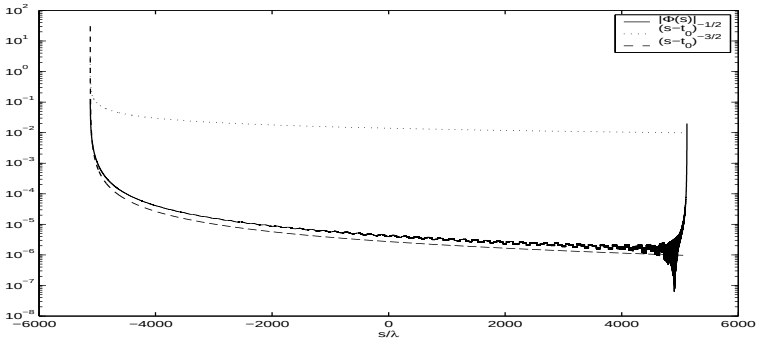

Figure 2: Plot of $|\Phi|$, $\varepsilon = 0.1$, $m = 5120$, so that $b - a = 10240\lambda$

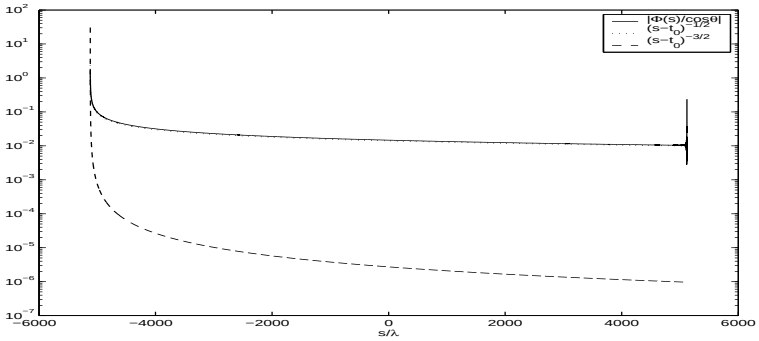

Figure 3: Plot of $|\Phi|$, $\varepsilon = 10^{-4}$, $m = 5120$, so that $b - a = 10240\lambda$

5 CONCLUSIONS

In this paper we have presented a Galerkin boundary element method for a problem of acoustic scattering by an unbounded surface with piecewise constant surface impedance, and we have demonstrated via both theoretical analysis and numerical examples that the number of degrees of freedom required for an accurate solution is bounded independently of the wavenumber. As the angle of incidence θ tends to $\pi/2$, i.e. at grazing angles, the number of degrees of freedom needed to maintain accuracy increases logarithmically with respect to $\cos\theta$.

References

[1] K Attenborough. Acoustical impedance models for outdoor ground surfaces. *J. Sound Vib.*, 99(4):521–544, 1985.

[2] S.N. Chandler-Wilde, S Langdon, and L Ritter. A high wavenumber boundary element method for an acoustic scattering problem. *Phil. Trans. R. Soc. Lond. A*, 2003. To appear.

[3] S Langdon and S.N. Chandler-Wilde. A Galerkin boundary element method for an acoustic scattering problem, with convergence rate independent of frequency. *Proc. Fourth U.K. Conf. on Boundary Integral Methods*, Salford University Press, 2003. To appear.

[4] S Langdon and S.N. Chandler-Wilde. A wavenumber independent boundary element method for an acoustic scattering problem. Isaac Newton Institute for the Mathematical Sciences Preprint NI03049-CPD, 2003.

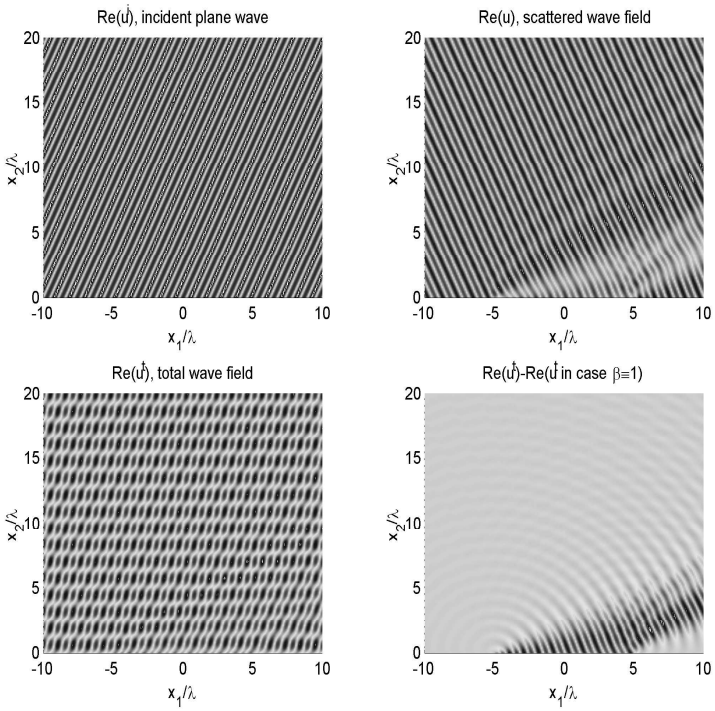

Figure 4: $m = 5$, $\varepsilon = 0.4$, results computed with $N = 16$

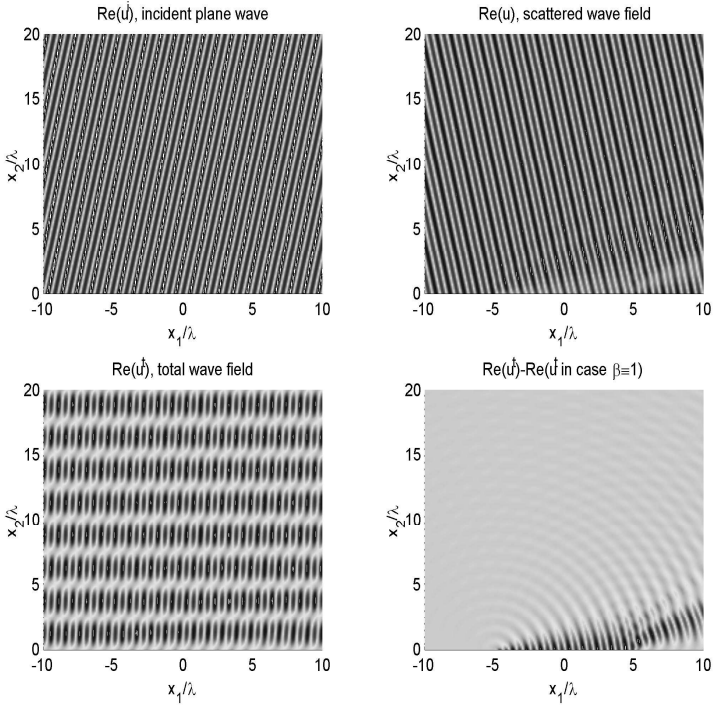

Figure 5: $m = 5$, $\varepsilon = 0.2$, results computed with $N = 16$

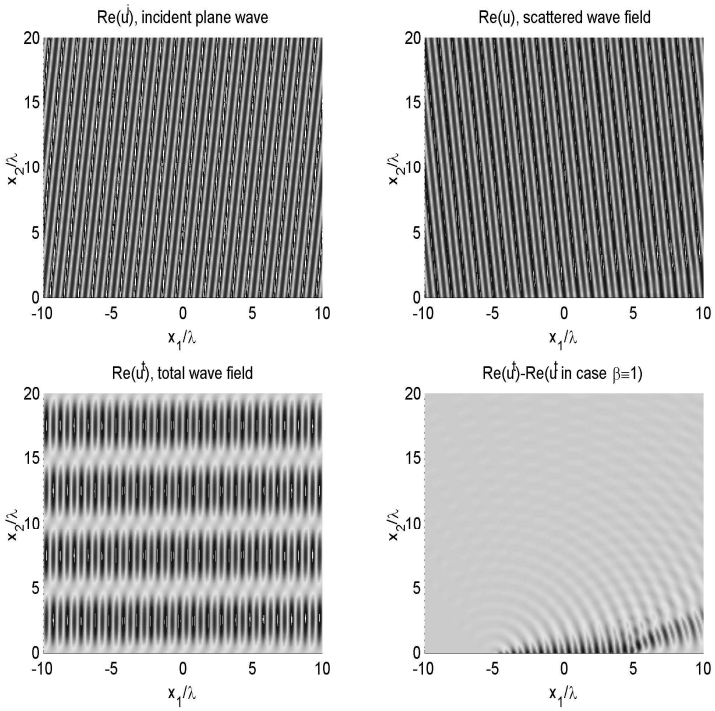

Figure 6: $m = 5$, $\varepsilon = 0.1$, results computed with $N = 16$

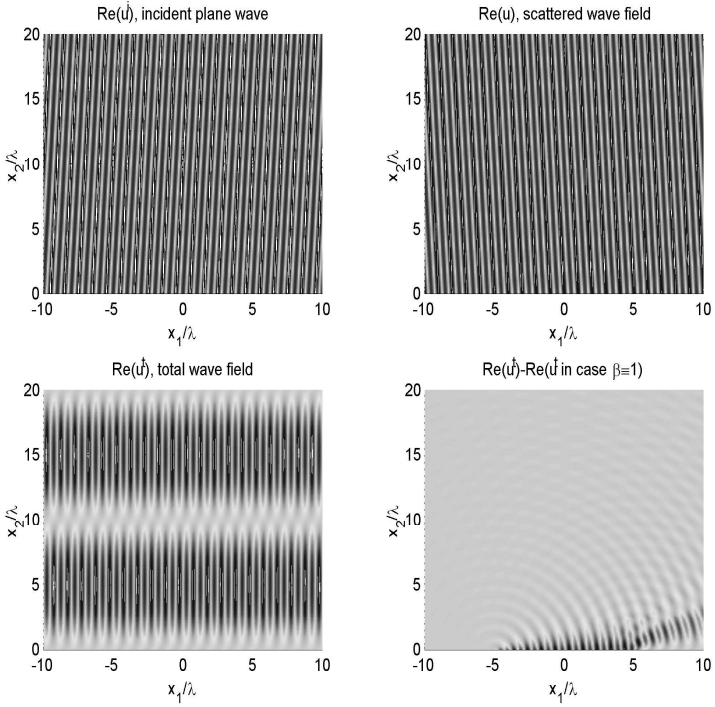

Figure 7: $m = 5$, $\varepsilon = 0.05$, results computed with $N = 16$

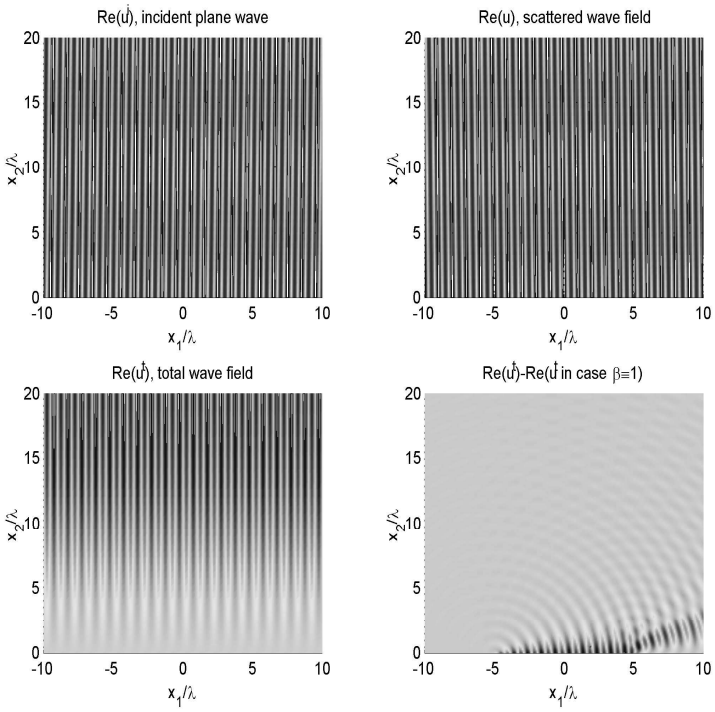

Figure 8: $m = 5$, $\varepsilon = 0.01$, results computed with $N = 16$

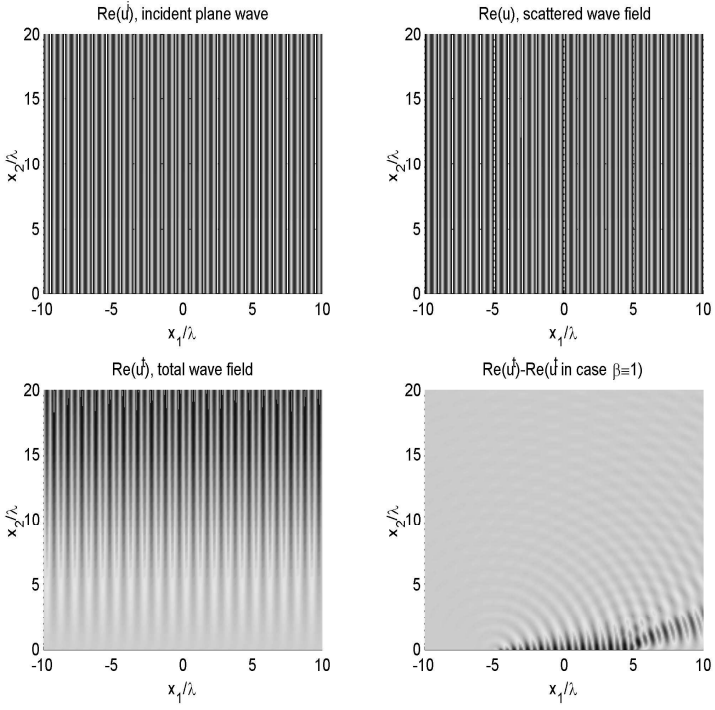

Figure 9: $m = 5$, $\varepsilon = 10^{-4}$, results computed with $N = 16$